Observation of transient lattice vacancies produced during high-energy ion irradiation of Ni foils

2007 J. Phys.: Condens. Matter 19 136205

(http://iopscience.iop.org/0953-8984/19/13/136205)

IOP PUBLISHING JOURNAL OF PHYSICS: CONDENSED MATTER

J. Phys.: Condens. Matter **19** (2007) 136205 (8pp) doi:10.1088/0953-8984/19/13/136205

Observation of transient lattice vacancies produced during high-energy ion irradiation of Ni foils

Hidetsugu Tsuchida[1,7], Takeo Iwai[2], Misa Awano[3], Mutsumi Kishida[3], Ichiro Katayama[4], Sun-Chang Jeong[5], Hidemi Ogawa[3], Naoki Sakamoto[3], Masao Komatsu[6] and Akio Itoh[1]

[1] Quantum Science and Engineering Centre, Kyoto University, Uji 611-0011, Japan
[2] Nuclear Professional School, School of Engineering, The University of Tokyo, Ibaraki 319-1188, Japan
[3] Department of Physics, Nara Women's University, Nara 630-8506, Japan
[4] Department of Materials Science, Japan Atomic Energy Research Institute, Ibaraki 319-1195, Japan
[5] Institute of Particle and Nuclear Studies, KEK, Tsukuba 308-0801, Japan
[6] Department of Intelligent Machine Engineering, Hiroshima Institute of Technology, Hiroshima 731-5193, Japan

E-mail: tsuchida@nucleng.kyoto-u.ac.jp

Received 20 October 2006, in final form 13 February 2007
Published 12 March 2007
Online at stacks.iop.org/JPhysCM/19/136205

Abstract

Real-time positron annihilation spectroscopy has been applied for the first time for the investigation of lattice vacancies produced during ion irradiation. Measurements were performed for thin nickel foils irradiated with 2.5 MeV C ions. Doppler broadenings of positron annihilation γ-rays were measured alternately during beam-on and beam-off conditions. It was found that the Doppler broadening line-shape parameter measured during irradiation is larger than those obtained before and after irradiation. This evidently implies that transient or non-survivable vacancy defects are produced during ion irradiation. On the other hand, no such significant change in the line-shape parameter was observed for other face-centred-cubic metal forms of aluminium.

1. Introduction

Studies of ion irradiation effects on materials have recently received considerable attention and a great deal of effort has been devoted to elucidation of radiation damage. Most studies have focused on how the radiation defect causes a change in material properties and structural modification of materials. For this purpose, new approaches such as studying the time evolutions of radiation damages or their *in situ* observation have been extensively explored in recent investigations [1–4].

[7] Author to whom any correspondence should be addressed.

Experimental investigations of ion-induced defect characteristics have been mainly carried out by means of an *in situ* observation system of a transmission electron microscope (TEM) combined with an irradiation system with fast ions from an accelerator [2, 3]. By using a real-time video-recording observation it is possible to make a visual investigation of ion-induced defect structure development relevant to clustering of defects occurring on timescales above a few tens of milliseconds.

Irradiation of fast ions is known to produce surplus point defects above thermal equilibrium concentrations in a nanometre-sized region near an ion trajectory (collision cascade region). The excess defects produced in a collision cascade are known to reveal the following relaxation phase sequence: cooling, thermalization, and diffusion [4]. The defects annihilate and agglomerate via interactions with one another, and with other various sinks such as dislocations, grain boundaries, and a surface. As a consequence, the recombination of point defects tends to reduce the number of primary displacements produced initially in a collision cascade.

The number of surviving defects is an important factor for determining final damage states. A program code TRIM [5] is widely used for calculating damage distributions and for estimating the total number of displacements produced per incident ion, i.e., displacements per atom (DPA). It is, however, well known that the number of displacements calculated from this code is larger than the actual number of surviving displacements, because defect-recombination processes are not taken into consideration in the TRIM code [6]. On the other hand, molecular dynamics (MD) computer simulations provide information about a variety of defect phenomena occurring in collision cascades in time and space including defect evolution, dynamics of recombination, and final defect states. Several MD simulations [7, 8] have demonstrated that the number of surviving defects (self-interstitial atom–vacancy pairs) is well below theoretical values calculated from the Norgett–Robinson–Torrens (NRT) formalism [9]. Depending on the irradiation temperature and the kinetic energy of primary knock-on atoms, the fraction of surviving defects is estimated to 10–40% of the number of displacements predicted by the NRT calculation. MD simulation results also show that the defects produced in a collision cascade mostly recombine within picoseconds.

At present little is known experimentally about the concentration of defects during irradiation with fast ions. In this paper, we report for the first time experimental results on lattice–vacancy behaviour during fast-ion irradiation explored by *in situ* positron annihilation spectroscopy. Positron annihilation spectroscopy is a powerful technique with a high sensitivity to vacancy-type defects, enabling us to examine an observable change of defect concentration as low as 10^{-7} [10].

The positron annihilation Doppler broadening spectroscopy was also performed simultaneously during ion irradiation of thin-foil specimens by using a specially developed experimental system combined with a slow-positron-beam apparatus and a high-energy ion accelerator. The aim of the present study is to obtain knowledge concerning the vacancy produced during irradiation. We measured real-time variation of line-shape parameters of positron annihilation spectra for two fcc materials of Ni and Al.

2. Experimental details

Experiments were carried out at the High Fluence Irradiation Facility of the University of Tokyo (HIT). Details of the apparatus used have been given in [11]. The experimental system makes it possible to observe *in situ* vacancies in materials produced in an ion irradiation environment. As a target specimen, a Ni foil was chosen because Ni has an interesting characteristic of vacancy mobility: vacancies in Ni are immobile at near room temperature (RT), while in many other metals they have some mobility at RT [12]. Kiritani *et al* have reported that vacancies

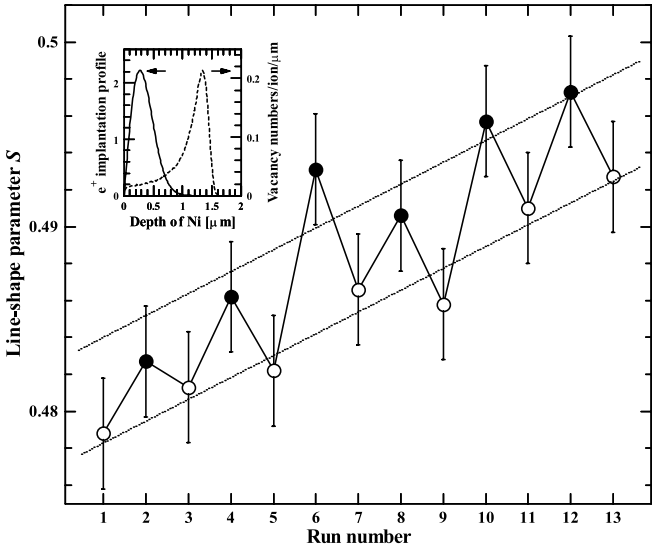

Figure 1. Variation of the S parameter measured sequentially during ion irradiation (closed symbols) and non-irradiation (open symbols) for a rolled Ni foil of 1.25 μm thickness irradiated with 2.5 MeV C ions observed with a positron beam of 15 keV. The inset shows the positron implantation profile and the number of vacancies produced by one incident ion (calculated from TRIM), as a function of the specimen depth. The dotted line is drawn as a visual aid.

in Ni become mobile at about 520 K [13]. On the other hand, vacancies in Al are mobile at RT. We examined polycrystalline foils of 1.25 and 2 μm thickness (light tight foils) of Ni and Al, respectively. Both foils were made by rolling. Annealing treatment was not carried out. The specimen was mounted on a target holder, self-supporting. A 2.5 MeV C^+ ion was used as a projectile, and its projected range is comparable to the foil thickness, so that changes in physical properties of the target specimen resulting from ion implantation can be avoided. Ion irradiation experiments were performed at a room temperature without controlling the specimen temperature. Therefore, the specimen temperature was measured during irradiation.

Ion beams above 15 mm in diameter were incident on a target at 30° to the surface normal, and a monoenergetic positron beam (below 30 keV) was directed parallel to the surface normal, where the target size was 13 mm in diameter. The spot size of the positron beam was about 10 mm in diameter on the target, and its beam intensity was about 10^4 s^{-1}, measured by a microchannel plate detector with a phosphor screen. Thus, the spot size of the positron beam is smaller than that of the ion beam, so that annihilation of the probing positrons occurs only in an ion irradiated area.

A Doppler broadening spectrum of positron annihilation γ-rays, measured with a high-purity Ge detector, was characterized by the line-shape parameter S defined as the ratio of counts in the central region of the annihilation photopeak (ranging from 510.2 to 511.8 keV) to the total counts of the peak (from 507.0 to 515.0 keV). The count of the annihilation γ-ray spectrum was about 6×10^4 for each measurement of the S parameter. Overall experimental errors of the S parameter were ± 0.003; these are mainly statistical errors.

3. Results and discussion

Figure 1 shows experimental results for the sequential variation of line-shape parameters S for Ni observed under beam-on (solid circles or even-numbered runs) and beam-off (open

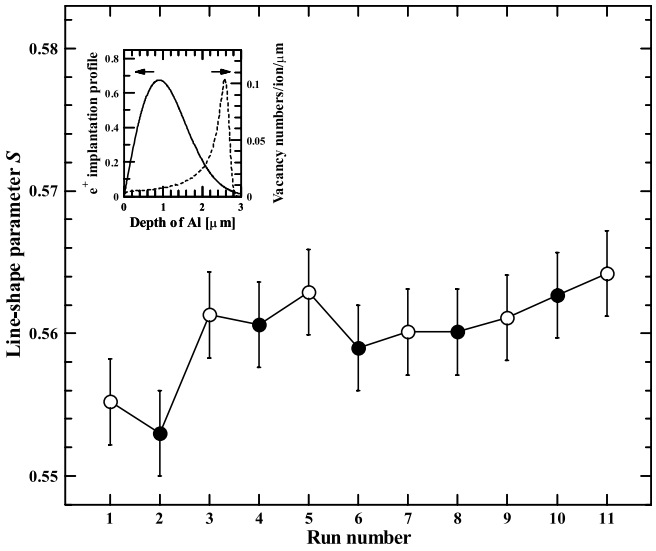

Figure 2. *S* parameter variation measured sequentially during ion irradiation (closed symbols) and non-irradiation (open symbols) for a rolled Al foil of 2 μm thickness irradiated with 2.5 MeV C ions. The inset shows the implantation profile for 15 keV positrons and the number of vacancies produced by one incident ion as a function of the specimen depth.

circles or odd-numbered runs) conditions which change alternately. We chose an incident positron energy of 15 keV in order to study defect development in a region of a uniform defect distribution produced by ion irradiation. To see the propagation characteristic of ions and positrons in a specimen, we made TRIM calculations [5] of the average number of vacancies produced by one incident ion as a function of the target depth (defect distribution). Also, the positron implantation profile at 15 keV was calculated from the formula based on the Makhov profile [14]. Calculated results are shown in the insets of figures 1 and 2 for Ni and Al, respectively. In calculation of the position implantation profile, we used the Makhov profile parameters of $A = 4.0\ \mu\text{g cm}^{-2}\ \text{keV}^{-1.6}$ and $m = 2$, determined by Vehanen *et al* [15]. The calculation shows that the implantation profile for 15 keV positrons overlaps in the region of nearly uniform defect distribution. In each run of annihilation spectrum measurements, the data acquisition time was 10 min, and the average fluence of ion beams was $\sim 1.7 \times 10^{14}$ ions cm^{-2} (where the average flux was $\sim 2.8 \times 10^{11}$ ions cm^{-2} s^{-1}).

One can see an obvious increase in S observed during ion irradiation (S_{during}). Experimental values of S_{during} are clearly larger than those measured just before and after irradiation, denoted by S_{before} and S_{after}, respectively, showing $S_{\text{during}} > S_{\text{after}} > S_{\text{before}}$. The difference between S_{before} and S_{after} arises from the different amounts of accumulation of surviving vacancies. With increasing fluence of ion beams, the S parameters measured under non-irradiation conditions increase from 0.479 (run 1, as received) to 0.493 (run 13) after irradiation with about 1.0×10^{15} ions cm^{-2}.

We measured the temperature of the specimen during ion irradiation. In real-time observation of the S parameter shown in figure 1, measurements of specimen temperatures were not carried out, in order to completely avoid positron annihilation originating from interaction with materials other than the specimen. The measurements were performed separately with a K-type fine gauge thermocouple of about 13 μm diameter (Omega Engineering Inc., USA) using a 1.7 MV tandem accelerator of Quantum Science and Engineering Centre, Kyoto University.

We measured specimen temperatures at the centre of the ion-beam spot as a function of the ion-beam flux. The flux was varied from 2.4×10^{10} to 4.7×10^{11} ions cm^{-2} s^{-1}. The thermocouple was covered carefully with a copper plate to avoid direct hits of ions. We found that the specimen temperature increases linearly with increasing flux and was about 400 K at 2.8×10^{11} ions cm^{-2} s^{-1}. At this temperature, vacancies are immobile because they become mobile at about 520 K.

The same measurements of S parameters were performed for Al foils under the same experimental conditions as for Ni. Results are depicted in figure 2, significantly different from those for Ni. S_{before} and S_{after} are nearly the same within experimental errors. This material dependence of the S parameter behaviour is probably due to the following two factors. One is the mobility of vacancies. It should be noted again that vacancies in Al are mobile, but not in Ni at the temperature of the present experimental condition. Vacancies may escape to sinks, leading to prevention of defects accumulating. This leads to non-variation of the S parameter under beam-on and beam-off conditions, as shown in figure 2. The other factor is formation of vacancy clusters. In fcc metals a vacancy cluster in the shape of stacking fault tetrahedra (SFT) is formed by irradiation. Numerous studies have demonstrated that stable SFT are formed in Ni, but not in Al [16, 17]. The stability and formation of SFT depend on the stacking fault energy and the shear modulus of the material [17]. Thus, it is likely that the formation of SFT eventually results in entirely different variations of the S parameter for Ni and Al.

Here, we discuss the increase of S occurring during ion irradiation. It is well known that the Doppler broadening parameter S contains information about the type (or size) and the density of vacancies at positron annihilation sites. Moreover, there is clearly a correlated relationship, showing S to increase with increasing vacancy size [18]. As described above, the present results show that S_{during} is larger than S_{after} observed just after the irradiation measurement under the beam-off condition. This suggests that some vacancies during irradiation are transient or non-survivable, and then recombine with mobile interstitials or pre-existing defects. The factors causing an increase in S during irradiation include (1) a higher concentration of vacancies and (2) formation of larger-sized vacancy clusters, compared with those of vacancies that have survived after irradiation.

We examined whether the variation of the S parameter observed for Ni (figure 1) is attributable to the effect of irradiation heating. As mentioned before, the measured temperature of the Ni during irradiation is about 400 K. We measured the variation of S caused by heat in the temperature range from 300 K (RT) to 573 K. Specimens were mounted on the copper plate, and were heated by a halogen lamp equipped with a temperature-control system in vacuum below 10^{-5} Pa. Specimen temperatures were measured with a thermocouple. In order to create a situation similar to the specimen temperature variation caused by alternative irradiation conditions, specimens were alternately controlled to several different temperatures at RT and higher temperatures (373, 473, and 573 K). At each temperature the S parameter was measured. Results are shown in figure 3. Values of S are found to be almost constant in a range 300–473 K within experimental errors and S starts to decrease at around 573 K. Since at the temperature of 573 K, vacancies in Ni become mobile, the decrease in S may be due to an annealing effect on a pre-existing defect. From these results we conclude that the irradiation heating effect is not an important factor in the increase of S under the present experimental conditions.

In runs 1 and 13 shown in figure 1, we performed measurements of the S parameters as a function of the positron incident energy E or the specimen depth, and obtained an S–E curve. In figure 4, measured values of S in run 1 become constant independently of the depth, indicating that positron trapping sites exist at any depth. This is probably due to the specimen used containing some defects such as dislocations arising from rolling. On the other hand, S in run 13 is found to become larger on approaching the sample surface, and to be larger than that

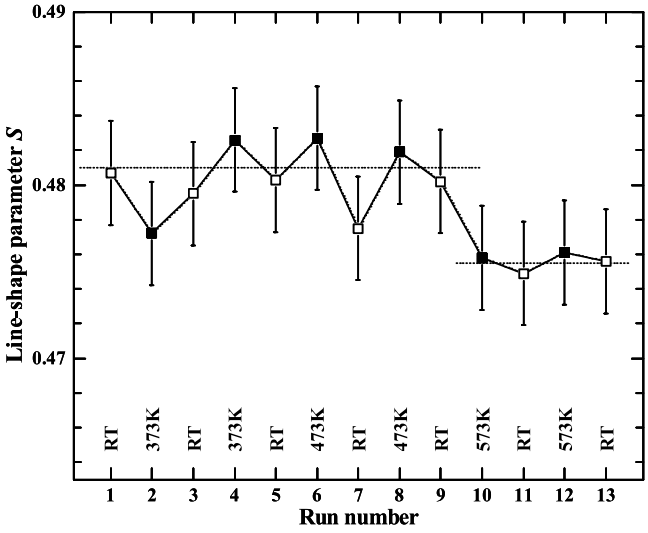

Figure 3. Temperature dependence of the *S* parameter variation due to a sequential heating for a non-irradiated Ni foil. The dotted line is drawn as a visual aid.

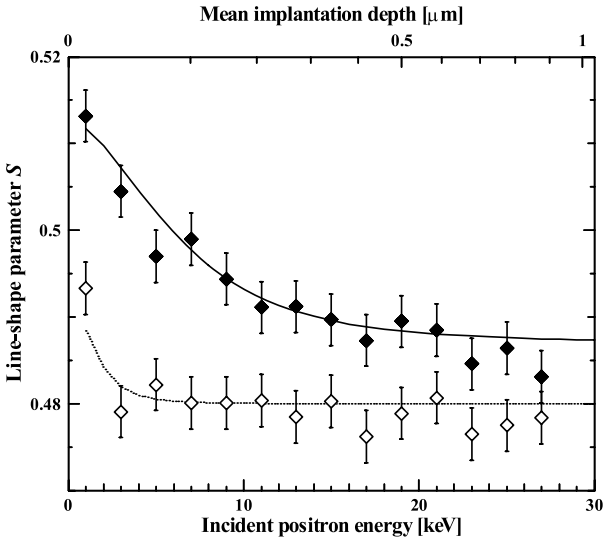

Figure 4. Positron annihilation line-shape parameter *S* as a function of the incident positron energy for the non-irradiated Ni foil (the first run in figure 1) and the Ni foil irradiated at a fluence of about 1.0×10^{15} ions cm^{-2} (the last run in figure 1); they are denoted by open and closed symbols, respectively. The dotted and solid lines are fitting curves according to a back-diffusion model for the first run and the last run, respectively (see the text).

in run 1 at the same positron energy. The result of run 13 suggests that positron trapping sites are produced predominantly near the surface.

The positron diffusion length was estimated from the *S*–*E* curve results following the back-diffusion model developed by Britton *et al* [19]. This model is a simple two-state model: positrons implanted into matter annihilate either at the surface or in the bulk, and this is based on the assumption that defects are distributed uniformly in matter. When a positron is implanted

into a solid, it rapidly loses its kinetic energy until it becomes near a thermal energy. After thermalization some positrons diffuse back to the surface. The fraction back-diffusing to the surface as a function of the incident positron energy, E in keV, is given by

$$F(E) = \int_0^\infty P(z, E) \exp(-z/L)\, \mathrm{d}z, \tag{1}$$

where L the diffusion length of positron and z the depth. $P(z, E)$ is the positron implantation profile which can be expressed as $P(z, E) = mz^{m-1}/z_0^m \exp[-(z/z_0)^m]$ with $z_0 = AE^n/(\rho\Gamma(1+1/m))$, where ρ is the mass density of material and Γ the gamma function. The measured S parameter as a function of E is expressed as

$$S(E) = S_\mathrm{s}F(E) + S_\mathrm{b}(1 - F(E)). \tag{2}$$

S_b is the value of the line-shape parameter for annihilation in a bulk region at a high incident positron energy and S_s the value for annihilation in a surface region. In the estimation, the average value of S measured in the energy range from 19 to 27 keV was regarded as S_b, and S_s was taken as the value of S measured at 1 keV. The value of $\rho = 8.90$ g cm^{-3} for Ni and the Makhov profile parameters of $A = 4.0\ \mu$g cm^{-2} keV$^{-1.6}$, $m = 2$, and $n = 1.6$ [15], were used. We obtain the value of L by fitting the data to equations (1) and (2). The fitting result is shown in figure 4. The value of L was estimated as about 10 nm for run 1 (before ion irradiation) and about 100 nm for run 13 (after ion irradiation), indicating that the diffusion length after irradiation is longer than that before irradiation. However, the value of L (=100 nm) is not reasonable because ion irradiation leads to the formation of defects and consequently the positron diffusion length becomes shorter due to defect trapping of positrons. Indeed, since the value of S for run 13 is larger than that for run 1 at the same positron energy, vacancy defects of a higher concentration are formed by ion irradiation for run 13. The S–E relationship of run 13 indicates that there is a gradient in the concentration of vacancies, i.e., the amount of vacancy defects increases with decreasing depth. When such a concentration gradient exists, the back-diffusion model described above is not applicable to calculation of the positron diffusion length because the mode is based on the assumption that the defect distribution is uniform.

The measurement for run 13 shows that vacancies of a higher concentration were formed at the surface region, implying that a surface influences the accumulation of vacancies. A similar result is reported in several investigations [20–22]. Kiritani and co-workers have studied the number of surviving defect clusters depending on the specimen depth for irradiation of Ni foils with neutrons at various temperatures ranging from 298 to 673 K [21, 22]. The result showed that the formation of vacancy clusters increases with decreasing depth. This is due to the fact that a freely migrating interstitial produced in a collision cascade escapes dominatingly to the surface: a surface sink effect for interstitials. Thus, the effect leads to the occurrence of vacancy clusters near the surface. Since vacancies are immobile, whereas interstitials are mobile under the present experimental conditions, it is likely that the surface sink effect occurs and vacancy clusters are dominantly formed in the surface region. In a phenomenological conclusion, an increase in S at lower E may be attributed to the formation of vacancy clusters.

4. Conclusions

In summary, vacancy defects produced during ion irradiation were studied by using an irradiation system combined with a slow-positron apparatus and a high-energy ion accelerator. For two fcc metals of Ni and Al, *in situ* positron annihilation Doppler broadening measurements were performed during irradiation and non-irradiation. We found that an increase in the S parameter occurs during irradiation for Ni, but not for Al. The result for Ni strongly suggests

that vacancy concentration during irradiation is high compared to that survived after irradiation, i.e., it includes transient or non-survivable vacancies. The formation of such a transient vacancy will be closely related to processes of defect accumulation or defect clustering.

The present *in situ* observation technique is demonstrated to serve as a powerful tool for the investigation of vacancies produced in materials under an ion irradiation environment. The Doppler broadening line-shape of positron annihilation radiation is known to provide comparative information but less information about defect characteristics such as the density and the open volume size. In contrast, positron lifetime measurements allow obtaining quantitative information. We plan to do further experiments on *in situ* positron lifetime measurement during ion irradiation of materials in order to obtain more accurate insights into the dynamics of irradiation effects, in particular a quantitative understanding of vacancy characteristics induced transiently during irradiation.

Acknowledgments

We would like to deeply thank Dr Michio Kiritani who motivated us to start the present study. We acknowledge Takao Omata and Jyunya Karimata for their technical assistance, and gratefully thank Professor Toshimasa Yoshiie and Dr Nagayasu Ohshima for their useful comments and discussion. This work was supported partly by the REIMEI Research Resources of Japan Atomic Energy Agency.

References

[1] Tsuchida H, Katayama I, Jeong S C, Haba M, Ogawa H, Sakamoto N, Mori H, Lee J G and Itoh A 2004 *Phys. Rev.* B **70** 054112
[2] Ishino S 1997 *J. Nucl. Mater.* **251** 225
[3] Birtcher R C, Kirk M A, Furuya K, Lumpkin G R and Ruault M-O 2005 *J. Mater. Res.* **20** 1654
[4] Ishino S 1993 *J. Nucl. Mater.* **206** 139
[5] Zieglar J, Biersack J F and Littmark U 1985 *The Transport of Ions in Matter (TRIM) Monte-Carlo Calculation Including in Computer Program SRIM Version 2003* (New York: Pergamon)
[6] Nastasi M, Mayer J W and Hirvonen J K 1996 *Ion–Solid Interactions: Fundamentals and Applications* ed D R Clarke, S Suresh and I M Ward FRS (Cambridge: Cambridge University Press)
[7] Singh B N and Zinkel S J 1993 *J. Nucl. Mater.* **206** 212
[8] Bacon D J, Gao F and Osetsky Yu N 2000 *J. Nucl. Mater.* **276** 1
[9] Norgett M J, Robinson M T and Torrens I M 1975 *Nucl. Eng. Des.* **33** 50
[10] Schultz P J and Lynn K G 1988 *Rev. Mod. Phys.* **60** 701
[11] Iwai T, Ito Y and Koshimizu M 2004 *J. Nucl. Mater.* **329–333** 963
[12] Ehrhart P, Jung P, Schultz H and Ullmaier H 1991 *Landolt–Börnstein Numerical Data and Functional Relationships in Science and Technology* Group III, vol 25 *Atomic Defects on Metals* ed O Madelung, p 202
[13] Kiritani M, Konno M, Yoshiie T and Kojima S 1987 *Mater. Sci. Forum* **15–18** 181
[14] Makhov A F 1961 *Sov. Phys.—Solid State* **2** 1942
[15] Vehanen A, Saarinen K, Hautojärvi P and Huomo H 1987 *Phys. Rev.* B **35** 4606
[16] Satoh Y, Yoshiie T, Mori H and Kiritani M 2004 *Phys. Rev.* B **69** 094108
[17] Schäublin R, Tao Z, Baluc N and Victoria M 2005 *Phil. Mag.* **85** 769
[18] Hakala M, Puska M J and Nieminen R M 1998 *Phys. Rev.* B **57** 7621
[19] Britton D, Rice-Evans P C and Evans J 1988 *Phil. Mag. Lett.* **57** 165
[20] Ishino S, Fukuya K, Muroga T, Sekimura N and Kawanishi H 1984 *J. Nucl. Mater.* **122/123** 597
[21] Kiritani M, Yoshiie T and Kojima S 1986 *J. Nucl. Mater.* **141–143** 625
[22] Yoshiie T, Kojima S, Satoh Y, Hamada K and Kiritani M 1992 *J. Nucl. Mater.* **191–194** 1160